6th International Trends in Welding Research Conference Proceedings, 15-19 April 2002, Pine Mountain, GA, ASM International, 2003

Finite Element Prediction of Residual Stresses in a Fillet Welded T-joint

Aihui Wu **Stavros Syngellakis** **Brian Mellor**
School of Engineering Sciences, University of Southampton, UK

Abstract

Welding-induced residual stresses and distortion can play a very important role in the reliable design of welded joints and welded structures. However, general simple methods for the prediction of the distribution and magnitude of residual stresses are not available from the literature. A reliable and efficient numerical analysis of this complex phenomenon can thus be considered as the only feasible alternative. A finite element (FE) simulation of a sequential fillet welding process producing a T-joint is presented in this paper. The main features of the essentially 2D analysis are ramped heat input function, temperature-dependent material properties and element death and re-birth technique. A parallel experimental investigation allowed the assessment of plastic properties variations in the welding area. Temperature history and welding-induced distortion data from tests were compared to the results from the FEM simulation for calibration and validation purposes. The validated model can be used to study the sensitivity of its predictions to variations of parameters such as heat input, material properties, radiation and fit-up. The final objective is to establish a reliable and versatile analytical tool for obtaining not only qualitatively but also quantitatively the welding-induced residual stresses and distortion. This information is essential to both researchers and designers for assessing the failure behaviour of welded joints and structures.

Introduction

Residual stresses may cause significant initial distortion leading to mismatching or buckling of slender welded structural elements. Magnitudes of residual stresses possibly up to yield stress level would greatly affect the fatigue crack initiation and crack growth rate in the region where tensile residual stresses develop. Through thickness residual stresses may cause lamellar tearing in thick-section weldments. To take into account the effect of the residual stresses in assessing crack-like flaws at a weld toe using fracture mechanics techniques, accurate predictions of the residual stress distribution across the plate thickness are required. There are, however, no generally applicable direct methods for the determination of the distribution and magnitude of residual stresses. Their experimental measurement is expensive, in most cases destructive and may be affected by many error sources. A reliable and efficient numerical analysis of this complex phenomenon can thus be considered as a more desirable alternative method.

Over the past two decades, the finite element method (FEM) has been used in several attempts to predict distortion and residual stresses due to welding. A welded T-joint is one of the most commonly used types of joints encountered in engineering practice. FEM simulations of the fillet welding process for T-joints have been presented in the literature. However, these models were either representative of only single-fillet weld joints[1,2] or based on the assumption of simultaneous welding on the two sides[3,4,5]. Apparently, no modelling work has been carried out on the sequential welding of the two fillet welds although this is what usually happens in engineering practice. The complexity of the modelling process may have contributed to this apparent lack of analytical results. In this paper, thermal and structural FEM models of a sequentially welded two-sided T-joint were generated and the corresponding welding process simulated. A parallel experimental investigation was also carried out in order to obtain accurate measurements of material properties in the welding area for the FEM model as well as temperature histories and distortion data, which were compared to results from the FEM simulation for calibration and validation purposes. A symmetric FEM model, representing simultaneous fillet welding on both sides of the weld, was also developed and run under identical conditions in order to assess the effect of sequential welding on residual stress. Through further comparison with published analytical experimental data, the developed simulation method is shown to be a reliable and versatile analytical tool for obtaining not only qualitatively but also quantitatively the welding-induced residual stresses and distortion. The validated model will be further used to assess the effect of various parameters such as

welding speed, thermal boundary conditions, material properties and fit-up on residual stress developed after welding

Experimental investigation

Welding process

A plate attachment of nominal dimensions 120×500×11.86 mm was joined to a main plate of nominal dimensions 260×500×11.86 mm by two single-pass fillet welds. Both plates were made of steel according to BS 4360: 1986 grade 43A. MIG welding process was used with BS 290 pt1:A18 solid mild steel MIG wire. The weld leg length and the fit-up gap were measured to be 5.8 mm and 0.5 mm, respectively. The geometry of the joint is illustrated in Fig. 1. K-type thermocouples were spot-welded to the plate surface to measure the temperature development during the welding and cooling process. A HP data logger was used to collect the temperature results digitally. During the welding process, the welding arc voltage and current were measured using an ISO-Tech ICM37 clamp multimeter; the welding time for the two passes and the interval between the passes were also recorded using a stop watch. The welding speed was approximately equal to 2 mm/s. After the specimen had cooled down to room temperature, the final distortion was measured.

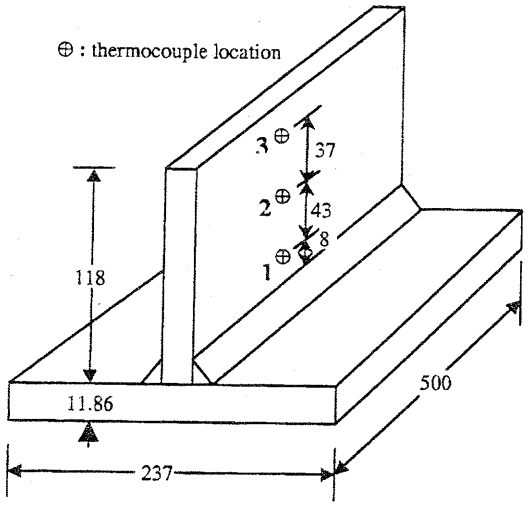

Fig. 1 Manufactured and analysed welded T-joint (all dimensions in mm).

Material property measurements

ASTM[6] standard rectangular tensile test specimens with a gauge length of 50 mm were manufactured from the steel plate and tested using an INSTRON 2511-320 machine to obtain the elasto-plastic stress-strain curve of the parent metal. Two round bar tensile specimens were manufactured from the weld and tested in an INSTRON machine with a 40% extensometer and the full stress-strain curve obtained. Both sets of data were converted to true stress-logarithmic strain curves, which are shown in Fig. 2. Because of the small area of the heat affected zone (HAZ) formed, it was not feasible for a tensile specimen to be taken from it; the plastic properties of the HAZ were thus deduced indirectly from micro-hardness test data.

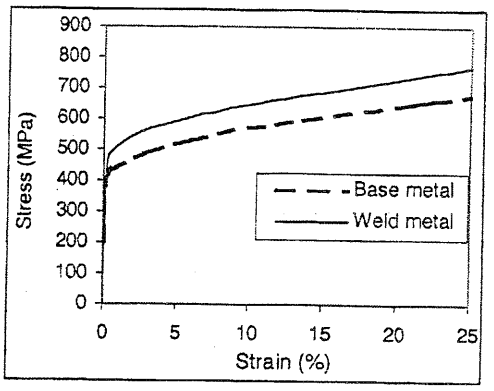

Fig. 2 Elasto-plastic properties of base and weld metal at room temperature.

Finite element modelling procedure

It has been recognised that the thermal and mechanical response of a weldment is a three-dimensional problem the solution of which is computationally expensive and very time-consuming. The problem has been simplified by assuming that, away from the ends of the plate, the majority of cross-sections are at a quasi-steady state so that a two-dimensional model of any such cross-section should lead to fairly accurate predictions of the thermal and mechanical behaviour of a three-dimensional joint[3,4].

In this paper, a 2-D thermal analysis was conducted first to obtain the global temperature history generated during the welding process. A stress analysis was then developed with the temperatures obtained from the thermal analysis entered as loading to the stress model. The general-purpose FE package ANSYS[7] was used for both thermal and stress analysis performed sequentially with the appropriate combination of elements. A decoupled thermal-stress analysis is commonly used in simulations of the welding process since the rather slow stress development affects very little the heat transfer process. Such an analysis is not only faster and computationally more economical, but also allows for all useful features of individual thermal and stress analyses available in FE packages to be applied.

The geometry of the FE model was identical to the cross-section of the tested specimen apart from the sizes and shapes of the two fillet welds, which were assumed to be the same in the FE model although they were slightly different in the specimen. Additionally, no overfill was included in the FE model. Fig. 3 shows the final FE mesh.

Thermal analysis

The non-linear transient heat flow analysis accommodated the temperature-dependent thermal properties and predicted the temperature development during the welding process. A four-node quadrilateral thermal solid element was used. The temperature-dependent thermal properties adopted were

mainly based on data reported by Brown and Song[2] which were compared with and found similar to those used by other investigators[3,8,9]. All the property-temperature relations used are shown in Fig. 4. The specific heat was converted to entropy input, which is favoured by ANSYS in the case of thermal processes involving phase changes.

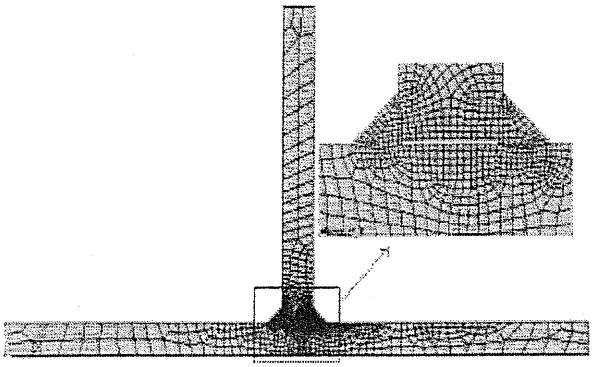

Fig. 3 Geometry and FE model

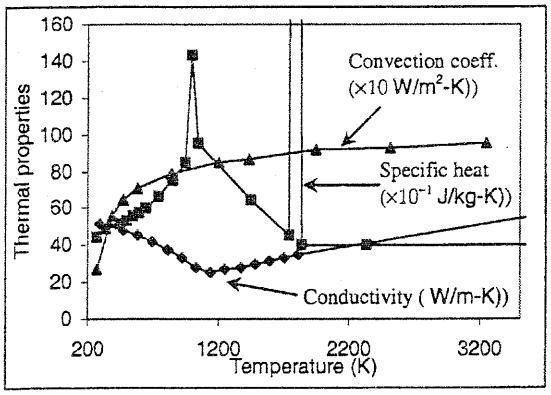

Fig. 4 Temperature-dependent thermal properties used in FEA

Heat source model

The total net heat input into the model, Q, was calculated from

$$Q = \eta VI \qquad (1)$$

where η is the arc efficiency, V the arc voltage and I the current. Thus Q was found approximately equal to 3.9 kW, which is equivalent to 19.34 kJ/cm for the welding speed applied. The total heat input was assigned to the model in the form of surface load Q_s and body load Q_b. Their ratio can be adjusted to achieve an accurate representation of the fusion zone. In this study, Q_s/Q_b = 0.175 was found to give temperature distributions that best fitted the fusion zone measured from the experiment. In the literature, various surface heat input models have been suggested and applied; these include the modified Gaussian and the ellipsoidal distributions. In this study, the surface heat flux was assumed to have a Gaussian distribution over the top surface of the weld metal and a short distance on the adjacent surfaces of the parent metal. The body heat generation rate Q_b was applied uniformly to the volume of the weld metal.

Initial and boundary conditions

In practice, the base metal is heated up from room temperature while the weld metal is fed into the work piece in a molten state with a temperature above the melting point. In previous analyses, the weld metal has been assumed to be initially at either room temperature[10] or melting temperature[2,10]. If room temperature is assigned as the initial temperature for the weld metal, part of the heat input is used to melt the electrode, i.e. to heat up the weld metal from room temperature. If the electrode temperature is initially set at its melting point, the heat input required must be subtracted from the total heat produced by the arc (more heat input propagates in the solid). In this paper, room temperature was used in the first instance as the initial temperature.

Convection was applied to all free surfaces of the specimen with a temperature-dependent heat convection coefficient as shown in Fig. 4. In order to account for the fact that the specimen was welded on top of a 35 mm thick steel plate through which heat was lost through conduction as well as convection, the convection coefficient for the bottom surface of the specimen was adjusted to include this effect. Furthermore, after the first pass on the right side has finished, the specimen will be distorted so that the left side of the specimen will not be in contact with the supporting plate and less heat will be conducted through it. After the second pass, the specimen tends to deform in the opposite direction so that, this time, part of the bottom surface on the right side of the specimen will leave the supporting plate. Thus the convection coefficient was varied during different stage of the welding process to account for these changes in real boundary conditions. The heat transfer between the surfaces of the attachment plate and the base plate, i.e. through the fit-up, was modelled using 2-D conduction bar elements.

Loading steps

In this 2-D simulation of an essentially 3-D welding process, the cross-section studied is somewhere in the middle region of the weldment transverse to the welding direction. Before the arc reaches the cross section analysed, the base metal of the section has already started to heat up due to the heat conducted from the part under the arc. Upon the arc reaching the position of the section, a large amount of heat is transferred from the arc directly to the section. When the arc leaves a section, this section is still receiving heat from the part under the arc through conduction. To include the effect of out-of-plane heat input as well as to avoid numerical divergence problems which may be caused by a sudden increase in temperature, Hong et al.[10] applied a ramped heat input function. This method was adopted in this study as well. The heat was input in four load steps for each pass as shown in Fig. 5, where $t_1 = t_3 = t_5 = t_7 = 1$ s, $t_2 = t_6 = 5$ s, $t_4 = 677$ s and $t_8 = 14{,}700$ s. These times roughly correspond to the welding and cooling periods measured during the welding of the test pieces. During pre-heat, the first pass weld area was considered absent and heat applied to the adjacent areas in the form of both surface heat flux and body heat. During the short

post-welding step, the previously applied surface and body heat load was assumed to linearly reduce to zero.

In most practical cases, the two sides of a T-joint are welded sequentially. In this study, this sequential welding process was simulated. As ANSYS does not allow the generation of new elements between load steps, the element death and rebirth features of the program were used to simulate the fact that during the first welding pass, the elements representing the second fillet weld do not exist. This element death and rebirth technique works in a way that the full model is generated first and those elements do not initially present are "killed" by multiplying their thermal and mechanical properties by a severe reduction ratio. Temperatures of those killed elements were constrained at room temperature until they were reactivated in later load steps.

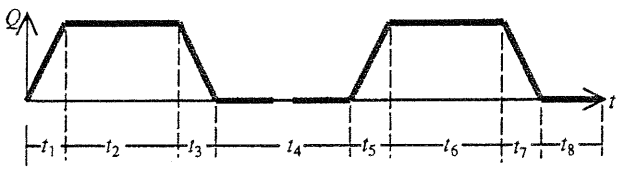

Fig. 5 Loading steps in the stress analysis

Stress analysis

A 2-D non-linear quasi-static stress analysis was subsequently conducted to calculate the welding-induced residual stresses. The thermal element was converted to the corresponding plane strain structural element available in ANSYS. Thus the mesh used in stress analysis was identical to that in the thermal analysis. It can be seen in Fig. 3 that this mesh is sufficiently refined in the weld and HAZ areas to capture stress variations due to significant temperature spatial gradients. The conduction bar elements through the fit-up gap were changed to 2-D node-to-node structural contact elements, which are only capable of supporting compression in the direction normal to the surfaces and shear in the tangential direction. The nodal temperature solutions obtained from the thermal analysis were read as loading into the stress analysis. In order to capture the residual stresses induced due to the heating and cooling cycle, the temperature history needed to be read at a sufficiently large number of time points, especially where the temperature gradient is large. The temperatures were read in load steps. However, the greater the number of the thermal solution steps used, the more the computational time and the larger the store space required. One way to improve efficiency is to identify the time points when the temperature gradient is low and remove some of the corresponding solution steps. The model was constraint at the middle of the bottom surface to prevent free-body movement.

The temperature-dependent Young's modulus and thermal expansion coefficient plots shown in Fig. 6 were based on relevant published data provided by various authors[2,3,5,9,10]. As mentioned earlier, the plastic properties of the base metal and the deposited weld metal at room temperature were experimentally determined. A multi-linear kinematic strain hardening model was adopted which was based on the stress-strain curves shown in Fig. 2. The temperature dependence of these properties was deduced by reference to similar information provided by other investigators[2,3,5]. A critical parameter, for which sufficient information could not be found in the literature, is the yield strain at high temperatures. Spurious plastic strains may be predicted if this quantity is not given a sufficiently high value. It was found that the residual stresses in the plane perpendicular to the welding direction are particularly sensitive to such plastic strains artificially generated in activated elements near or above the melting temperature.

The element kill and rebirth technique was used in stress analysis as well to simulate the deposition of each weld at the respective temperature loading step. Appropriate material property changes were also imposed between steps. The elements belonging to the first fillet weld were activated at the end of deposition phase ($t = t_1 + t_2$) to simulate the absence of the weld during pre-heat and its fluid state during deposition. The elements representing the second pass were also activated after the weld deposition through the section.

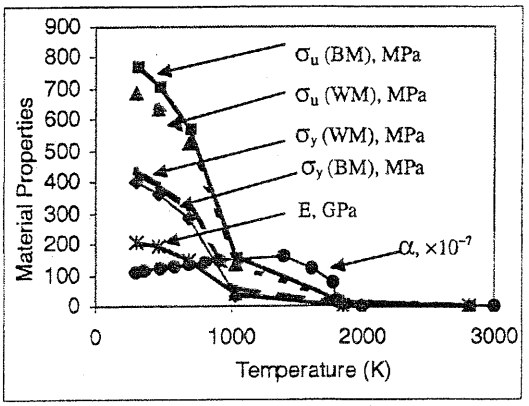

Fig. 6 Temperature-dependent mechanical properties used in FEA

Results and discussion

The temperature histories at thermocouple locations 1, 2, and 3 (Fig. 1), obtained from both the experiment and the FE analysis, are shown in Fig. 7. A good agreement between them has been achieved through the calibration of certain input parameters such as heat input and boundary convection, for which uncertainties arise regarding both their magnitude and distribution. Careful examination of the predicted temperature distribution over the weld and the area surrounding it at various critical stages of the simulation confirmed the validity of the solution. The fusion zone was, for instance, predicted within the expected limits.

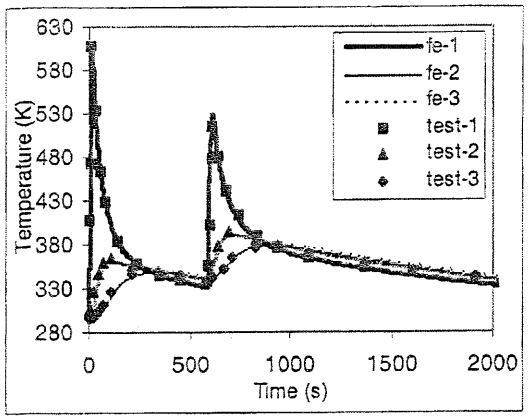

Fig. 7 Measured and predicted temperature histories.

The stress analysis results were monitored throughout the simulation in order to ensure a rational mechanical response to every stage of temperature input. Compressive stresses were observed in the heated areas counterbalanced by tensile ones away from them. This pattern was gradually reversed during cooling.

The final distortion of the test piece was measured to be 86.6°. This is comparable with the FE prediction.

The final residual stress are presented in Figs 8 to 11. Fig. 8 shows the longitudinal stress (σ_{zz}) distribution along the surfaces of the plate (a) and attachment (b). This was compared with patterns determined experimentally[11] and found to be in agreement.

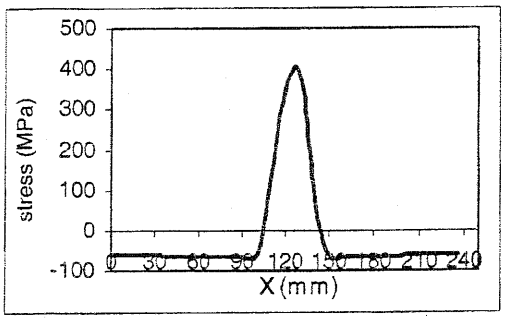

(a) Along bottom surface of the base plate

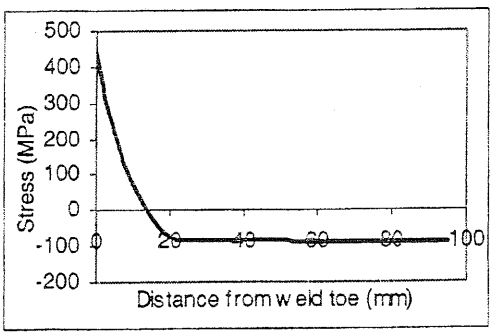

(b) Along left surface of the attachment plate

Fig. 8 Longitudinal residual stress patterns

The focus in the present investigation has been on the in-plane stress distribution, which can be associated with brittle or fatigue fracture if amplified by external action transmitted through the structure. The results for σ_{xx} in the first and the second pass fillet are presented in Figs. 9 and 10, respectively. For comparison with previous analyses[4], the simulation was repeated for the symmetric case of simultaneous welding on both sides. The result for σ_{xx} from that analysis is shown in Fig. 11.

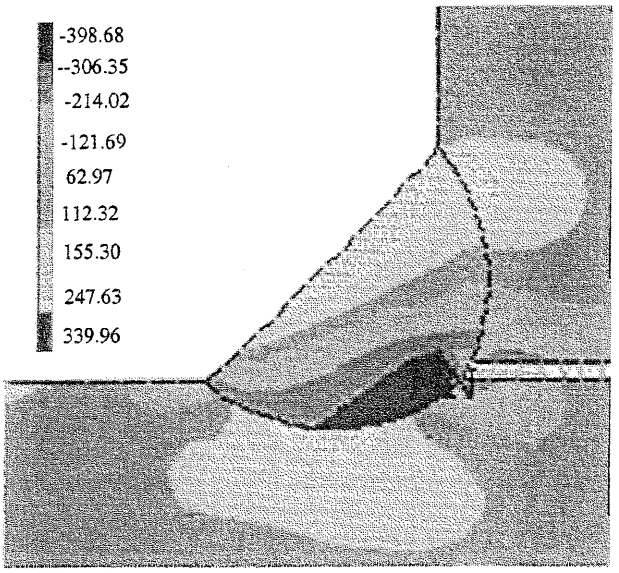

Fig. 9 In-plane residual stress σ_{xx} in the first pass weld

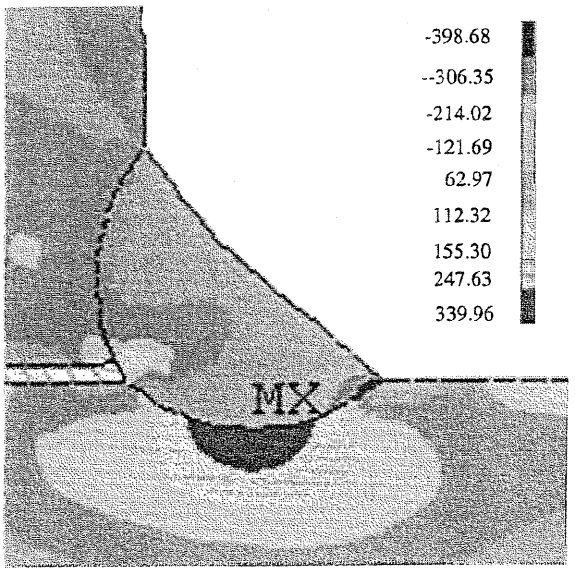

Fig. 10 In-plane residual stress σ_{xx} in the second pass weld

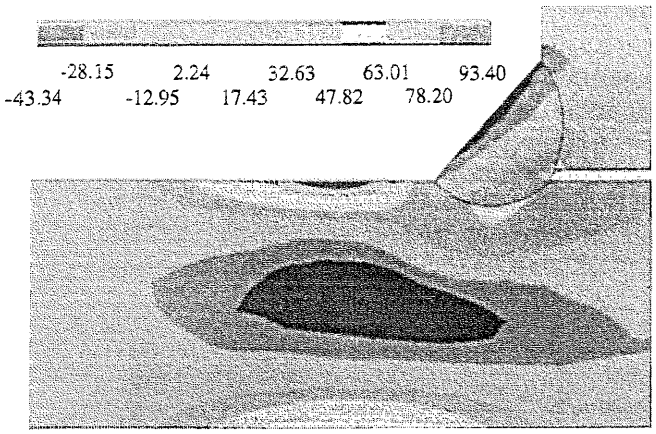

Fig. 11 In-plane residual stress σ_{xx} in the fillet weld for a symmetric process

The results for σ_{yy} are similar but rotated by 90°.

Conclusions

The FE simulation of the welding process presented in this paper provided some new information on the residual stress magnitude and distribution over the weld area of a T-joint. These numerical results are extremely difficult to verify experimentally due to the small size of the area of interest and the extreme environmental conditions prevailing during the process. Every effort was made however to ensure a rational correlation between developing stresses and the corresponding temperature history. It is thus evident that a reliable thermal analysis is a prerequisite to the accurate prediction of residual stresses.

Detailed predictions of residual stress distributions are required for assessing the fracture and fatigue behaviour of welded T-joints. Combining these solutions with analyses of the joints under various loading and constraint conditions could lead to local failure models, which would be incorporated into global structural FEM analyses.

Various modelling features can be explored in greater detail. These concern heat input distribution, initial as well as boundary thermal conditions. More detailed information on the temperature dependence of both thermal and mechanical properties is essential as shown by the sensitivity of the results to variations of such properties especially at high temperatures. Modelling of more complex phenomena such as phase transformation could be included in the developed simulation method so that their effects on results could be assessed.

Another important consideration is the variation of material properties within the heat affected zone (HAZ). A parallel experimental investigation based on instrumented micro-hardness tests is currently under way for the elasto-plastic characterisation of the HAZ. These data will eventually be entered to the developed FE simulation so that effect of HAZ on the local residual stress distribution could be assessed.

References

[1] S. Brown. And H. Song,, *Welding Res. Suppl.*, 71, 55s-62s (1992)
[2] S. Brown and H. Song, *J. Engin. Industry – Trans. ASME*, 114, 441-451 (1992)
[3] P. Michaleris and A. DeBiccari, *Welding Res. Suppl.*, 76, 172s-181s (1997)
[4] S. Sarkani, V. Tritchkov and G. Michaelov, *Finite Elem. Anals Desi.*, 35, 247-268 (2000)
[5] T-L. Teng , C-P Fung, P-H Chang and W-C Yang, *Int. J. Pres. Vessels and Piping*, 78, 523-538 (2001)
[6] ASTM Designation E 8M – 98: Standard Test Methods for Tension Testing of Metallic Materials (1998)
[7] ANSYS 5.6, SAS IP, Inc., Canonsburg, PA (1999)
[8] L. E. Lindgren, H. Runnemalm and M. O. Näsström, *Int. J. Num. Meth. Engineering*, 44, 1301-1316 (1999)
[9] M. Jonsson, L. Karlsson and L. –E. Lindgren, *J. Engin. Mat. Techn., Trans. ASME*, 107, 265-270 (1985)
[10] J. K. Hong, C.-L. Tsai and P. Dong, *Welding Res. Suppl.*, 372s-381s (1998)
[11] N. R. Nagaraja Rao, F. R. Estuar. and L. Tall, *Welding Res. Suppl.*, 295s-306s (1964)